Monatshefte für Chemie 133, 807–814 (2002)

Monatshefte für Chemie
Chemical Monthly

Self-Organization of Magnetic Nanoparticles and Inclusion of Hydrogen by Borohydride Reduction

Iovka Dragieva[1,*], **Christina Deleva**[1], **Mladen Mladenov**[1], and **Ivania Markova-Deneva**[2]

[1] Central Laboratory of Electrochemical Power Sources, Bulgarian Academy of Sciences, BG-1113 Sofia, Bulgaria
[2] Chemical Technology and Metallurgical University, BG-1756 Sofia, Bulgaria

Summary. Different structures of the interglobular space or voids between self-organized nanoparticles lead to differences in the measurable magnetic properties of single-domain particle chains of similar composition, grain size, and amorphous structure of the single globules. The volumes and radii of nanoparticles obtained by application of a magnetic field (3 to 15 nm) are larger than those determined without application of a magnetic field during the borohydride reduction process. Two types of hydrogen containing nanotubes with diameters of up to 2 (small-size containers) and 5 nm (large-size containers) are produced using as a driving force the domain wall formation energy between ferromagnetic nanoparticles with quantum size effected dimensions prepared by this reduction method at room temperature and ambient atmosphere. Nanoscale hydrogen containers can be used instead of *Me*H nanoparticle electrodes as perfect energy charge transfer media of high efficiency (close to 100%) using Li ion electrolytes. No influence on the electrode temperature and no participation of OH^- and H_2O in the main charge/discharge transfer reactions were observed.

Keywords. Self-organization; Ferromagnetic nanoparticles; Borohydride reductions; Charge transfer; Thermodynamics.

Introduction

The aim of this study is to continue our investigations on nanoscaled tubes formed from single-domain ferromagnetic nanoparticles produced by borohydride reduction, containing inside hydrogen clusters arranged as tubes or channels of different diameters (2 or 5 nm) [1, 2]. The possibility for application of these nanoscale tubes not as hydrogen storage elements or *Me*H electrode materials, but with regard to their application in Li ionic solid state batteries without participation of OH^- groups or H_2O in the main charge/discharge transfer reactions is discussed.

* Corresponding author. E-mail: iovka@cleps.bas.bg

Results and Discussion

Self-organization of nanoparticles in chains

The borohydride reduction process leads to the formation of single-domain (amorphous or crystalline [3]) nanoparticles whose shape, size, grain size distribution, structure, and magnetic and conductive properties depend on technological parameters such as metal salts used, complex-forming agents, time of mixing and hydrodynamic regime, *pH* value of the solutions used, application of a DC magnetic field during the reduction process, *etc*. The use of a magnetic field during the preparation of ferromagnetic amorphous nanoparticles by borohydride reduction produces no change in the kind of particles formed in terms of structure or shape, but affects the configuration of the interparticle space or voids of the chains obtained as a result of nanoparticles self-organization. Curling and buckling nets or chains built from single domain globules trap the hydrogen delivered during the borohydride reduction process into nano-dimensional cages [4]. The experimental data obtained from BET absorption isotherms show that depending on whether a DC magnetic field is applied or not, interglobular spaces of definite dimensions and structures appear [4]. Thus, irrespective of the presence of the closest packing of nanoparticles along the chains, the applied magnetic field decreases the void volume (the inside diameter of the channels filled with hydrogen is 2 nm), and as a result, the chain becomes denser. As established earlier [5–11], the different structures of the interglobular spaces lead to differences in the measurable properties of single-domain particle chains of similar composition, grain sizes, and magnetic amorphous structures of the single globules.

The basic element proposed for nanoparticle chains obtained in a DC magnetic field is a *pentahedron*, whose sixth globule (with flexible volume) is situated above the pentahedral level [5, 6, 8] and which exhibits a *tetrahedral* interparticle space (cross-sectional shape of hydrogen channels).

The basic element proposed for nanoparticle chains obtained in absence of a magnetic field is a *hexagonal* ring with the seventh globule incorporated in its center (on the same level with the remaining six surrounding globules [5]) and having an *octahedral* interglobular space.

Particles with radii smaller than 10 nm

As the particle size decreases towards some critical particle diameter, the formation of domain walls becomes energetically unfavourable, and the resulting species are called single-domain particles. Changes in the magnetization can no longer occur through domain wall motion and require the coherent rotation of spins instead. The activation volume of the cluster or of the nanoparticle is an estimate of the volume over which spins act coherently. Coherent rotation of all spins is assumed when the activation volume is smaller than the physical volume of the switching unit due to incoherent reversal mechanisms. One of the most interesting aspects of the behaviour of a nanometer size magnetic particle is the fact that the magnetic north and south poles may suddenly interchange due to quantum tunneling. In this case, the magnetic moment of the particles behaves as a quantum object rather than a

Table 1. Influence of DC magnetic field application during the synthesis of nanoparticles by borohydride reduction on grain size and content of hydrogen and boron [12]

Magnetic field	$(FeCo)_xB_yH_z$		$(SmCo_5)_xB_yH_z$		$(NiCo)_xB_yH_z$		$(Fe_2Si)_xB_yH_z$	
	no	yes	no	yes	no	yes	no	yes
$SSA/m^2 \cdot g^{-1}$	87	59	88	75	11	41	24	30
Particle radius/nm	5.7	8.5	7.2	8.6	47	12	26	21
Hydrogen content/at.%	0.27[a]	0.44[a]	27	29	18.1	12.5	11.2	16.9
Boron content/at.%	4.3[a]	3.6[a]	25.2	29.4	23.6	25.8	14.2	10.7
Number of atoms	–	–	$2 \cdot 10^5$	$4 \cdot 10^5$	$5 \cdot 10^7$	$1 \cdot 10^6$	$1 \cdot 10^7$	$6 \cdot 10^6$

[a] Data from Ref. [9]

classical vector. The two equivalent but opposite orientations of the magnetic moment are separated by an energy barrier which varies linearly with the volume of the particle. The cluster's magnetic moment is decoupled from the lattice and fluctuates thermally in direction, all orientations being equally favourable. When placed in a magnetic field, a nonzero-averaged magnetic moment develops and aligns with the applied external field [12].

Consequently, the measured volumes and radii of nanoparticles obtained under application of a DC magnetic field (Table 1) are larger than those of nanoparticles obtained in the absence of a magnetic field. In such spherical nanoparticles (*e.g.* from 3 to 15 nm; Table 1, $(FeCo)_xB_yH_z$ and $(SmCo_5)_xB_yH_z$), almost 50% of the atoms are on the surface of the particle, and coherent spins can aligns with the external magnetic field, thus increasing the measured volume of the single-domain particles.

Data published earlier have shown that the penetration of gaseous phases like ammonia in the case of gaseous nitrogenation of iron–boron nanoparticles through hydrogen channels with tetrahedral structure is slower and time limited at 400°C in comparison to the same process through hydrogen channels with octahedral structure or with a twice as large cross section (5 nm) [5]. It has also been proved that the smaller nanovoids (with diameters around 2 nm and filled with higher content of hydrogen) are elastic and cannot be subjected to 100 MPa press loading in contrast to the larger voids (5 nm, containing half the amount of hydrogen) [5, 9, 10, 11].

The different magnetic properties – higher coercive force, higher squareness, and lower magnetization (or the opposite) – for both kinds of chains were estimated from specific self-organization phenomena and differences in volume packing density (0.96 and 0.74, respectively, along the chains) [7, 9, 12]. Both types of chains can be included in magnetic lack coatings as longitudinal inside perpendicular to the surface (LIPS) oriented metal magnetic particle layers for high density hard disks production [12].

Thermodynamic analysis

Summarizing our experience on $Me_xB_yH_z$ nanoparticle preparation by borohydride reduction and their application as *Me*H electrodes [13, 14] tested with 6 *M* KOH

electrolyte, we decided to avoid the charge transfer between nanoparticle surfaces and electrolyte. The fundamental thermodynamic relationships determining the cell voltage and the basic types of electrode reactions in the case of hydrogen or charged hydrogen groups are as follows:

$$H + e^- \rightarrow H^- \tag{1}$$

$$H^- - e^- \rightarrow H \tag{2}$$

$$H - e^- \rightarrow H^+ \tag{3}$$

$$H^+ + e^- \rightarrow H \quad (\textit{Volmer}) \tag{4}$$

$$H + H \rightarrow H_2 \quad (\textit{Tafel}) \tag{5}$$

$$H^+ + e^- + H \rightarrow H_2 \quad (\textit{Heyrovsky}) \tag{6}$$

The driving force for all reactions is the difference between the standard *Gibbs* free energies of the products and those of the reactants [2]. The thus estimated data *vs.* temperature for reactions according to Eqs. (1) to (6) are shown in Fig. 1.

The probabilities of Eqs. (1), (3), (5), and (6) at room temperature and the required catalysts, temperature, or potentials for Eqs. (2) and (4) can be well estimated. To use the reversibility of the above reactions with a participation of hydrogen or charged hydrogen groups and to prepare *Me*H electrodes and produce batteries on that basis is a difficult technological problem with a high degree of complexity, especially in terms of water elimination.

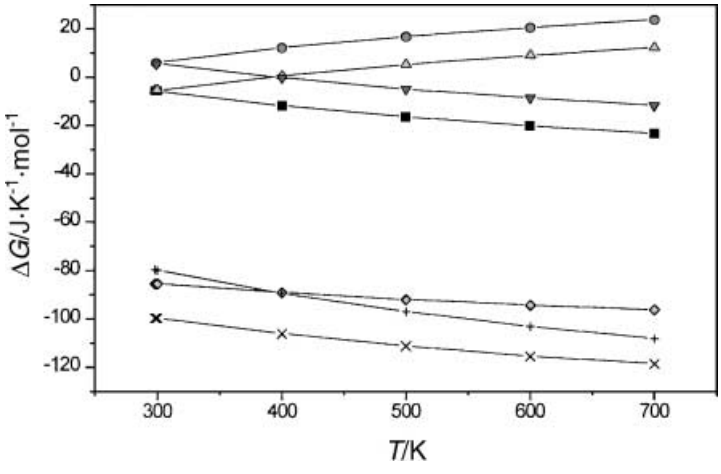

Fig. 1. Standard *Gibbs* free energies *vs.* temperature; Eq. (1): ■, Eq. (2): ●, Eq. (3): △, Eq. (4): ▼, Eq. (5): ◇, Eq. (6): +, Eq. (9): ×

Conclusions

Our hypothesis for the working model in the case of nanoscale hydrogen container (or ferromagnetic nanotubes for storage of hydrogen) applications in Li batteries is as follows:

(*i*) For the reactions taking place on the surface of the hydrogen storage magnetic nanotubes (or nanoscale containers for hydrogen), the charge carrier is the lithium ion according to Eqs. (9), (10), and (11) (cf. Experimental).
(*ii*) The character of the Li–H bond obtained as a result of the electrochemical reactions of stored hydrogen with $LiClO_4$ electrolyte through the net of single-domain nanoparticles is typically covalent, and charge/discharge potentials influence its formation and polarization.
(*iii*) The bond between lithium and hydrogen is stronger (bond strength: 238.049 kJ/mol) than that between lithium atoms (bond strength: 110.21 kJ/mol) [16], and the dispersion of lithium atoms on the nanotube surface is a real fact; however, they do not form pair junctions as thin films on the surface of nanoscaled containers.
(*iv*) Nanotubes filled with hydrogen can be applied as a perfect charge transfer energy media with very high efficiency (close to 100%) with no need of mass transfer of hydrogen or hydrogen containing atomic groups as has been proven for the case of Li ions as charge carriers.

The mechanism of charge/discharge of magnetic chains and nanotubes filled with hydrogen in non-aqueous electrolytes is presently being investigated by IR spectroscopy; first results are very promising.

Experimental

Nanoscale containers for hydrogen or hydrogen-filled channels inside ferromagnetic chains were prepared by the reduction of aqueous metal salt solutions with an aqueous solution of $NaBH_4$ according to Eqs. (7) and (8) [15].

$$NaBH_4 + 2H_2O \rightarrow NaBO_2 + 4H_2\uparrow \tag{7}$$

$$BH_4^- + 2M^{2+} + 2H_2O \rightarrow 2M\downarrow + NaBO_2 + 4H^+ + 2H_2\uparrow \tag{8a}$$

$$BH_4^- + H_2O \rightarrow B\downarrow + OH^- + 2.5H_2\uparrow \tag{8b}$$

Two types of hydrogen containers (small-size container: diameter up to 2 nm; large-size container: up to 5 nm) were produced using as a driving force the domain wall formation energy between ferromagnetic nanoparticles with quantum size effected dimensions prepared by borohydride reduction. Both types of containers are built up from single domain metallic nanoparticle nets, anisotropically self-organized, forming channels of different diameters at the inside with different content of hydrogen and different specific surface areas.

Experiments with aqueous electrolyte (6 M KOH)

The samples were prepared as electrodes by mixing nanoscaled particles (and hydrogen containers, respectively) with teflonized acetylene black (TAB-2) in a weight ratio of 50:50 as anodic and NiOOH as cathodic materials; Hg/HgO was used as a reference electrode. The experimental electrodes were

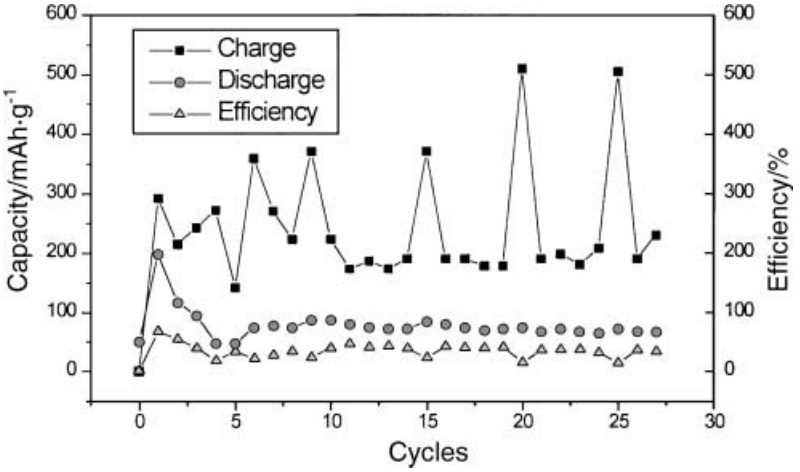

Fig. 2. Specific charge/discharge capacity and efficiency *vs.* cycle number for a small-sized hydrogen container as cathode in KOH electrolyte and NiOOH as anode

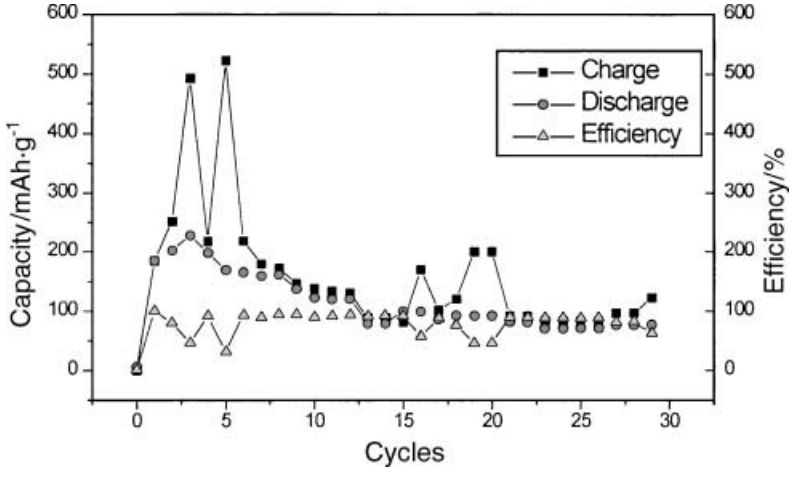

Fig. 3. Specific charge/discharge capacity and efficiency *vs.* cycle number for a large-sized hydrogen container as cathode in KOH electrolyte and NiOOH as anode

cycled upto 30 times in a laboratory 4-electrode glass cell at a current density of 74 mA/g (smaller hydrogen container) and 75 mA/g (larger hydrogen container).

Our experimental results shown in Figs. 2 and 3 indicate that the mechanism of the reactions on the *Me*H nanoparticle (and hydrogen storage nanotubes or containers) electrode surfaces in OH^- solutions (6 *M* KOH electrolyte) can be represented by Eqs. (4), (5), and (6). Between the two types of hydrogen containers, no difference can be detected in the charge/discharge cycling procedure in alkaline electrolyte.

Experiments with non-aqueous electrolyte (1 M $LiClO_4$)

We decided to find an alternative way to solve the thermodynamic and experimental problems encountered with water and aqueous electrolytes in *Me*H batteries. The estimated standard free energy

formation of a compound between lithium and hydrogen atoms makes the following reaction feasible:

$$\mathrm{Li} + \mathrm{H} \rightarrow \mathrm{LiH} \tag{9}$$

The reaction according to Eq. (9) shown in Fig. 1 is more preferable throughout the whole temperature range with respect to reactions according to Eqs. (5) and (6). Two more reactions (Eqs. (10) and (11)) of charge/discharge in the Li^+ electrolyte with regard to hydrogen containers may take place:

$$\mathrm{Li}^+ + \mathrm{e}^- \rightarrow \mathrm{Li} + \mathrm{H} \Rightarrow \mathrm{LiH} \tag{10}$$

$$\mathrm{LiH} - \mathrm{e}^- \rightarrow \mathrm{Li}^+ + \mathrm{H} \tag{11}$$

The samples were prepared according to Ref. [2] as experimental electrodes by mixing nanoscaled particles (and containers) with teflonized acetylene black (TAB-2) as a cathodic mixture in a weight ratio of 50:50 and Li metal as anodic material. A Li/Li^+ reference electrode and a non-aqueous electrolyte (*1 M* $LiClO_4$ in *PC + EC* (propylene carbonate : ethylene carbonate = 1:1, Fluka®)) were employed. The electrodes were separated by a glass fiber paper (Amer-Sill). The cathodes were prepared by pressing the cathode mixture onto Ni or Al foil disc collectors (15 mm). The probes were cycled up to 60 times as cathodes in special stainless lab cells fitted with a steel spring in order to maintain a definite pressure ($2.5\,\mathrm{kg \cdot cm^{-2}}$) on the electrode face and using $LiClO_4$ as electrolyte with a moisture content of up to 20 ppm. The cells were charged and discharged at a constant current of $74\,\mathrm{mA \cdot g^{-1}}$ of the active material (*cd*: $0.5\,\mathrm{mA \cdot cm^{-2}}$) to an upper limiting voltage of 4.20 V. When the limiting discharge voltage of 1.00 V was reached, the next cycle was started. The experimental results for both types of containers are shown in Table 2.

In the case of Ni foil, the smaller container working as a cathode had an initial discharge capacity. For the larger container, no initial discharge capacity could be detected experimentally. For the case of

Table 2. Specific charge (Ch.)/discharge (Disch.) capacity and efficiency (Eff.) *vs.* cycle number for small- and large-sized hydrogen containers as cathodes in $LiClO_4$ electrolyte

Number of cycling	Ni foil						Al foil					
	Small container			Large container			Small container			Large container		
	Capacity/mAh · g^{-1}						Capacity/mAh · g^{-1}					
	Ch.	Disch.	Eff./%	Ch.	Disch.	Eff./%	Ch.	Disch.	Eff./%	Ch.	Disch.	Eff./%
0	0	191	0	0	0	0	0	0	0	0	377	0
5	208	207	99	226	224	99	205	201	98	222	205	93
10	195	187	96	199	198	99	179	179	100	183	168	92
15	165	164	99	179	178	99	160	169	95	170	153	90
20	150	150	100	166	163	98	147	148	99	155	148	95
25	119	119	100	156	153	98	128	128	100	303	185	76
30	115	117	98	140	137	98	121	120	99	161	155	97
35	116	116	100	–	–	–	113	112	99	148	143	97
40	99	99	100	–	–	–	100	100	100	155	155	100
45	95	95	95	–	–	–	–	–	–	155	158	98
50	85	85	100	–	–	–	–	–	–	135	143	94
55	–	–	–	–	–	–	–	–	–	131	104	80
60	–	–	–	–	–	–	–	–	–	84	124	68
65	–	–	–	–	–	–	–	–	–	128	124	97

Al foils, contrary to Ni collector, the smaller container working as a cathode had no initial discharge capacity, whereas an initial discharge capacity was detected for the larger container. The efficiency of the charge/discharge capacity in both cases (Ni and Al foils) is more constant for the smaller container. However, a comparison of the specific capacities of the two samples (Al foils) at the 30^{th} cycle shows very similar or equal values as those obtained using Ni foils at the 25^{th} cycle (Table 2). At the 30^{th} cycle, the determined capacities for larger and smaller containers are close to 155 and 120 $mAh \cdot g^{-1}$, respectively.

Working with $LiClO_4$ electrolyte, a well-determined difference between the specific capacity of the larger nanoscaled hydrogen container in comparison to the capacity of the smaller nanoscaled hydrogen container was observed and estimated. The specific capacities are proportional to the respective specific surface areas of the containers, not to the content of hydrogen (in weight percents) or to the hydrogen density [4, 9, 10].

Acknowledgements

The authors want to express their gratitude to the management committee of COST 523 and personally to Prof. *H. Hofmann* for accepting Bulgaria among the member countries of this COST action and for contributions to the work of the Mid-Term Workshop held in Limerick, Ireland (October 2–6, 2001).

References

[1] Dragieva I, Mladenov M, Popov A, Stoynov Z (2001) In: Program of 22nd International Power Sources Symposium, Manchester, England, April 9–11, p 15
[2] Dragieva I, Deleva Ch, Mladenov M, Zlatilova P (2001) Lecture at NATO New Trends in Intercalation Compounds for Energy Storage, NATO Advanced Study Institute, Sept. 21–Oct. 2, Sozopol, Bulgaria (accepted for publication)
[3] Dragieva I, Klabunde K, Stoynov Z (2001) J Scripta Mater **44**: 2187
[4] Mehandjiev D, Dragieva I, Slavcheva M (1985) J Magn Magn Mat **50**: 205
[5] Dragieva I, Buchkov D, Mehandjiev D, Slavcheva M (1988) J Magn Magn Mat **72**: 109
[6] Mehandjiev D, Dragieva I, Slavcheva M, Buchkov D (1989) Comm Dep Chem **22**: 338
[7] Dragieva I, Mehandjiev D, Slavcheva M (1990) J Magn Magn Mat **83**: 460
[8] Dragieva I, Slavcheva M, Buchkov D, Mehandjiev D (1990) J Magn Magn Mat **89**: 75
[9] Dragieva I (1990) In: Emin D et al (eds) Boron-Rich Solids, AIP Conference Proceedings 231. Amer Inst Phys, Albuquerque, NM, p 516
[10] Nikolov S, Dragieva I, Buchkov D (1990) In: Emin D et al (eds) Boron-Rich Solids, AIP Conference Proceedings 231. Amer Inst Phys, Albuquerque, NM, p 294
[11] Mehandjiev D, Dragieva I (1991) J Magn Magn Mat **101**: 167
[12] Dragieva I (1999) In: Nedkov I, Ausloos M (eds) Nano-Crystalline and Thin Film Magnetic Oxides, NATO Science Series, 3. High Technology, 72, Kluwer, p 165
[13] Mitov M, Popov A, Dragieva I (1999) J Appl Electrochem **29**: 59
[14] Bliznakov S, Ivanova G, Dragieva I, Popov A, Stoynov Z (2000) In: Julien C, Stoynov Z (eds) NATO Science Series 3. High Technology, 85, Kluwer p 619
[15] Dragieva I, Slavcheva M, Buchkov D (1986) J Less Common Met **117**: 311
[16] Lide DR et al (eds) (1997–1998) Handbook of Chemistry and Physics, 78th edn. CRC Press, Boca Raton, New York, pp 9–55

Received October 25, 2001. Accepted (revised) January 3, 2002